

# Noise Mechanisms in Small Grain Size Perpendicular Thin Film Media

Jian-Gang Zhu, *Fellow, IEEE*, Vincent Sokalski, Yiming Wang, and David E. Laughlin

Data Storage Systems Center, Carnegie Mellon University, Pittsburgh, PA 15213 USA

In this paper, we present a set of systematic experimental investigations on possible noise mechanisms for current perpendicular thin film media of small grain sizes. In particular, we focus on intergranular exchange coupling and grain boundary surface anisotropy in the granular layer of the present continuous-granular-composite film structure. Micromagnetic modeling studies are conducted to study the impact of the observed experimental phenomenon. Modeled experiments show that significant intergranular exchange coupling may occur when oxide grain boundary thickness becomes less than 1 nm. If the grain boundary thickness has significant distribution below this critical value, the exponential dependence of the coupling strength on the oxide thickness would yield significant degradation of the medium signal-to-noise ratio. Carefully designed experiments have also been conducted to study possible grain boundary interfacial anisotropy. Co/Cr, CoPt/Cr, Co/SiO<sub>2</sub>, Co/Cr<sub>2</sub>O<sub>3</sub>, and Co/TiO<sub>2</sub> interfaces are investigated and the corresponding interfacial anisotropy strengths are quantitatively measured. Although Co/SiO<sub>2</sub> interfacial anisotropy appears to be the weakest among them, the measured interfacial anisotropy energy strengths for all of them are significant fractions of the crystalline perpendicular anisotropy of the grains at present grain sizes. Finally, we investigated the impact of stacking faults in *hcp* Co-alloy grains. It is found that when the anisotropy strength of a small segment of a grain substantially reduces due to the existence of stacking faults, it will yield a switching field reduction disproportional to the volume ratio of the segment.

*Index Terms*—Magnetic recording, medium noise, PMR media, stacking faults, thin film media.

## I. INTRODUCTION

**R**EDUCTION of noise has become more critical than ever in increasing area storage density capability in current hard disk drives (HDDs). In this paper, we present a systematic combined experimental and micromagnetic modeling study in an attempt to obtain some in depth understanding of possible medium noise mechanisms in current perpendicular magnetic recording (PMR) media.

The magnetic storage layer in current PMR thin film media consists of two magnetic layers: a layer of magnetic CoCrPt grains separated by oxide grain boundaries (referred to as the granular layer or oxide layer) capped by a layer of CoCrPt alloy grains (stacked on top of grains in the oxide layer) without oxide (referred to as the capping layer). The two magnetic layers are usually separated by a thin metallic layer serving the function of achieving adequate interlayer coupling. Such a structure was first proposed as the continuous-granular-composite (CGC) structure [1]. One of the features offered by the CGC structure is that intergranular exchange coupling can be optimized by adjusting the thickness ratio between the granular and capping layers since the capping layer offers spatially uniform intergranular exchange coupling while no intergranular exchange coupling should occur in the oxide layer due to the oxide grain boundaries.

Increasing the number of grains per unit surface area has been identified as the route to reach the constant moving area density target. However, over the past couple of years, attempts to decrease the center-to-center distance between adjacent grains in perpendicular media have failed to show the expected medium signal-to-noise ratio (SNR) gain. This prompted us

to conduct an experimental study on the possible intergranular exchange coupling in the granular layer. It is found that significant intergranular exchange coupling could occur when the oxide grain boundary thickness becomes less than 1 nm. A distribution of grain boundary thickness below this critical value would yield a significant distribution of the intergranular coupling field, causing large transition noise, as shown in this paper. After our initial experimental and micromagnetic studies, film media in some of the newly released high area density HDD products actually show relatively thick oxide grain boundaries, leading to a slight increase of the average center-to-center grain separation in recent months [2].

Another mechanism which also could cause switching field dispersion is the interfacial anisotropy arising from the magnetic grain boundary interfaces. Since the easy axis of this grain boundary surface anisotropy is orthogonal to that of the perpendicular anisotropy within the grain, a large grain boundary surface to volume ratio would yield significant reduction of the magnetic switching field of the grains. Furthermore, the fact that this switching field reduction is grain size dependent implies that a distribution of grain size will lead to a distribution of the magnetic switching field. In this paper, we also present an experimental study which attempts to quantitatively determine the interfacial anisotropy in perpendicular thin film media.

The third medium noise mechanism studied here is possible stacking faults (SF) within the magnetic grains in the media. Experimental studies indicated that SFs in *hcp* Co-alloy film could yield significant reduction of the perpendicular anisotropy strength. A micromagnetic study presented in this paper investigates the possible impact of SFs in terms of switching field distribution.

## II. EXCHANGE COUPLING IN GRANULAR LAYER

Fig. 1 shows a transmission electron microscopy (TEM) micrograph of the granular layer of a commercial perpendicular thin film disk (with approximately 250 Gbits/in<sup>2</sup> density capability). Note that oxide grain boundary varies from grain to

Manuscript received August 30, 2010; accepted September 02, 2010. Date of current version December 27, 2010. Corresponding author: J.-G. Zhu (e-mail: jzhu@ece.cmu.edu).

Color versions of one or more of the figures in this paper are available online at <http://ieeexplore.ieee.org>.

Digital Object Identifier 10.1109/TMAG.2010.2076330

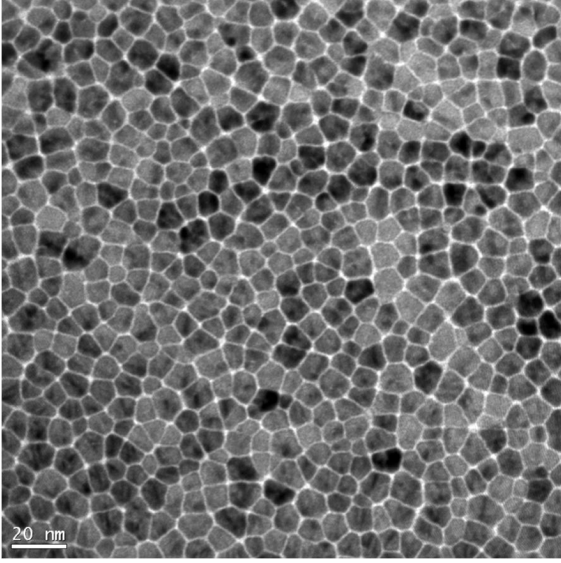


Fig. 1. A transmission electron microscopy micrograph of the granular layer in a commercial hard disk drive disk medium. The thickness of the oxide grain boundaries evidently varies from grain to grain.

grain. To quantitatively understand the extent of the intergranular exchange coupling through the oxide grain boundaries in the granular layers, a modeled experiment has been conducted [3], [4].

By creating a CoPt/oxide/CoPt trilayer thin film stack, the interlayer exchange coupling between the two CoPt layers through the oxide interlayer could be obtained by measuring the dependence of the magnetization switching on the oxide layer thickness. Using a single crystalline MgO substrate with (110) texture, we epitaxially grow a pseudo single crystal Cr layer with (112) texture by sputtering at an elevated substrate temperature of 400°C. Subsequent growth of a 24 nm thick Co<sub>84</sub>Pt<sub>16</sub> layer on top of the Cr layer at room temperature yields a *hcp* structure for the CoPt layer with (10.0) texture. Since the CoPt layer has a single *c*-axis orientation in the film plane, a relatively high coercivity was achieved even though the film is completely continuous. The second Co<sub>84</sub>Pt<sub>16</sub> layer deposited on top of the oxide interlayer is 8 nm thick, shows no particular texture, and is magnetically soft relative to the bottom oriented, and therefore magnetically hard, CoPt layer.

The distinctive coercivity difference between the two CoPt layers enables the determination of the exchange coupling through the oxide interlayer. Fig. 2 shows a series of measured hysteresis curves for Cr<sub>2</sub>O<sub>3</sub> interlayers of various thicknesses. The minor loops in these curves correspond to the magnetization switching of the top soft Co<sub>84</sub>Pt<sub>16</sub> layer. The lateral shifts of the minor loops at thin oxide layer thickness arise from the interlayer exchange coupling, whose energy density can be obtained from

$$\sigma = H_{\text{shift}} \cdot M_{s,\text{soft}} \cdot \delta_{\text{soft}} \quad (1)$$

where  $M_{s,\text{soft}}$  and  $\delta_{\text{soft}}$  are the saturation magnetization and the thickness of the soft CoPt layer, respectively.

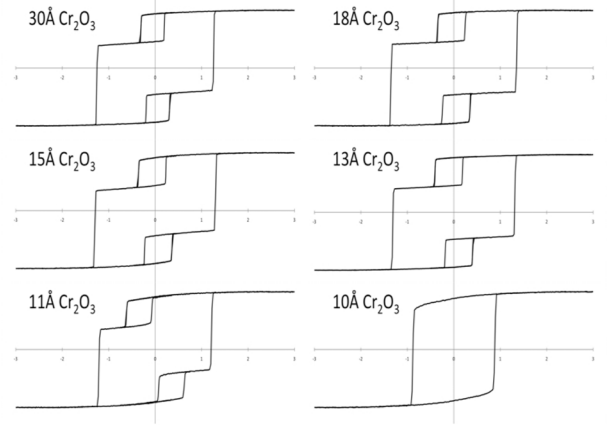


Fig. 2. A series of measured hysteresis curves for the MgO/Cr/CoPt/Cr<sub>2</sub>O<sub>3</sub>/CoPt film stack of various thickness of the Cr<sub>2</sub>O<sub>3</sub> (target composition) interlayer. The minor loop corresponds to the switching of the top soft CoPt layer and its lateral shift arise from the interlayer exchange coupling through the Cr<sub>2</sub>O<sub>3</sub> interlayer.

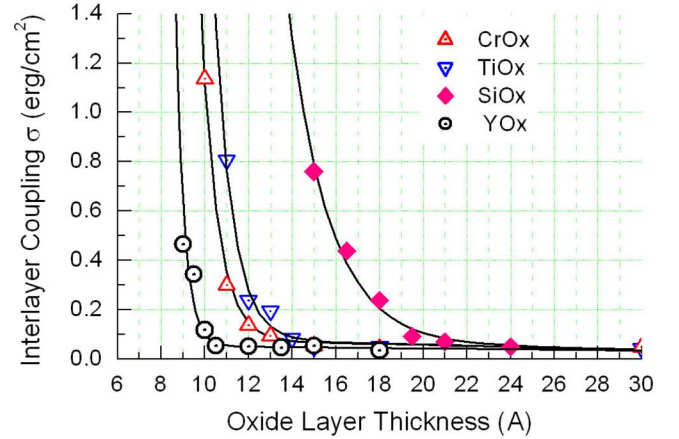


Fig. 3. Measured interlayer exchange coupling energy densities as a function of the interlayer thickness for a variety of oxides.

Fig. 3 shows the measured interlayer exchange coupling energy density as a function of the interlayer thickness for a variety of oxide materials. Among them, SiO<sub>x</sub> appears to be the worst and YO<sub>x</sub> the best in terms of minimum thickness needed to eliminate the interlayer exchange coupling. The measurement data shown here do not seem to be very dependent on deposition conditions. It is our belief that the measured coupling energy dependence on the interlayer thickness is very much a characteristic of the oxide material. Furthermore, the oxide layers are found to be relatively smooth and continuous, even at thicknesses less than 1 nm, as a fairly representative TEM cross-section micrograph shown in Fig. 4.

In practice, the magnetic grains in the granular layer are made of CoCrPt alloy material and there is experimental evidence of Cr segregation to grain boundaries [5]. To investigate the effect of Cr segregation on intergranular exchange coupling, we performed the following additional experiments: very thin Cr layers, 1.0–1.5 Å, were deposited prior to, as well as subsequent to, the deposition of the oxide layer. Such interfacial “dusting” of pure Cr was performed for both TiO<sub>x</sub> and SiO<sub>x</sub> layers, the

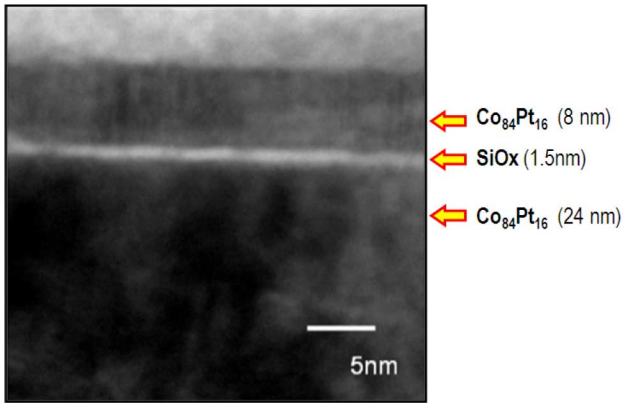


Fig. 4. Cross-section TEM image showing CoPt layers with a 1.5 nm  $\text{SiO}_x$  interlayer.

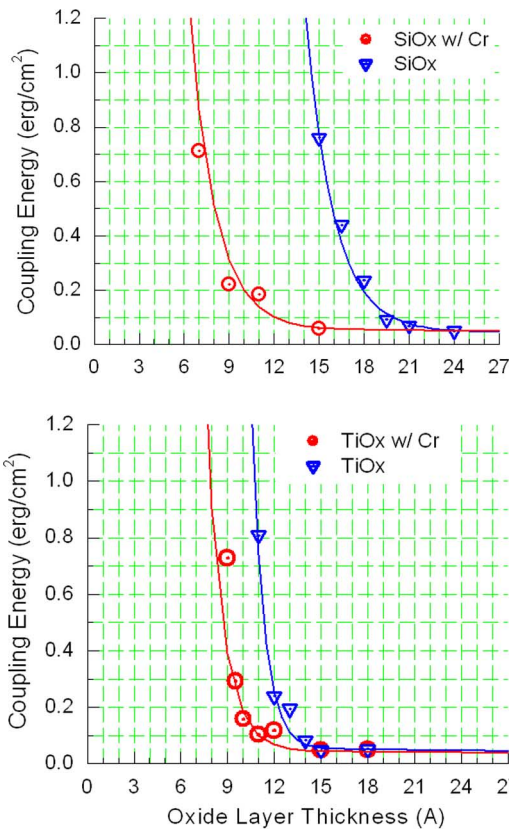


Fig. 5. Comparison of the coupling energy density with and without Cr dusting at the CoPt oxide interfaces for  $\text{SiO}_x$  (upper) and  $\text{TiO}_x$  (lower).

two most commonly used oxide materials in present commercial perpendicular media. Fig. 5 shows the measured interlayer coupling energy densities for the Cr dusting on  $\text{SiO}_x$  and  $\text{TiO}_x$  layers, respectively. In the case of a  $\text{SiO}_x$  layer, with the Cr dusting, the coupling versus oxide layer thickness curve shifts by almost 8 Å. The thickness shift is significantly greater than the added Cr thickness. In the case of  $\text{TiO}_x$ , the shift is significantly smaller as compared with the  $\text{SiO}_x$  interlayer. Note that the resulting critical thicknesses of the two oxide layers after the Cr dusting become very similar, even though they are very different without the Cr dusting.

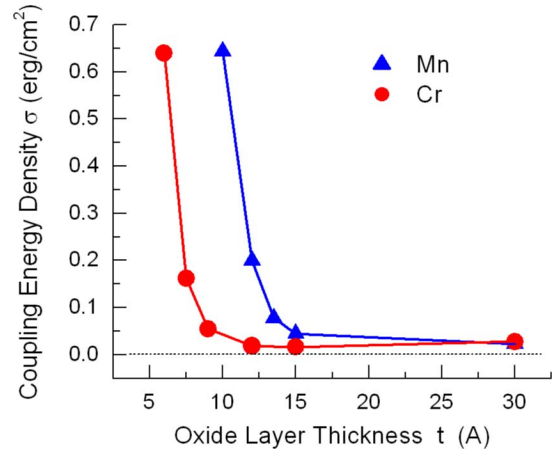


Fig. 6. Measured interlayer coupling energy density as a function of the interlayer thickness for interlayer materials being Cr (red circle) and Mn (blue triangle).

Two metallic interlayers were also studied. Fig. 6 shows the measured coupling energy density as a function of interlayer thickness for the interlayer being solely Cr (red) and solely Mn (blue), respectively. Among all the interlayers studied here, Cr appears to be most effective in terms of eliminating/reducing the interlayer exchange coupling.

Even though the formation of oxide grain boundaries in the granular layer of present perpendicular disk media could be different from the formation of the oxide interlayer in these modeled experiments, the results presented here should be very relevant, especially if the exchange coupling is dominated by the oxide material characteristics. It would be difficult to imagine that the morphological quality of the grain boundary oxide layer would be better than the oxide layer formed in our modeled experiments, in which case the results presented here would provide the best scenario in terms of exchange decoupling between nearest neighboring grains.

Examining Fig. 5, it can be seen that if the granular layer of a medium possesses a significant distribution of grain boundary thickness below 1 nm, the distribution of intergranular exchange coupling strength could become substantial. Micromagnetic modeling has been performed to provide quantitative understanding on the impact of medium signal-to-noise ratio (SNR) [5]. The perpendicular medium is modeled by two layers of magnetic grains. A two layer CGC medium structure is modeled. The top capping layer is 4 nm thick and the bottom granular layer is 12 nm. Spatially uniform exchange coupling is assumed in the capping layer with exchange coupling constant  $A = 0.6 \text{ erg/cm}^3$ . The saturation magnetization of the capping and granular layers is 460 emu/cc and 520 emu/cc, respectively. The anisotropy field of the capping layer is 7.9 kOe while that of the granular layer is 10.7 kOe. The easy axes deviation is assumed to be 3 degrees and the anisotropy field dispersion is 3%. The two layers are exchange coupled with coupling energy density  $4 \text{ erg/cm}^2$ . A wrap around shield head is used throughout the recording process. The pole width is 55 nm and the bevel angel is 10 degrees. The head has a write gap width 35 nm and side shield gap width 70 nm. The recording field is simulated by commercial finite element method (FEM)

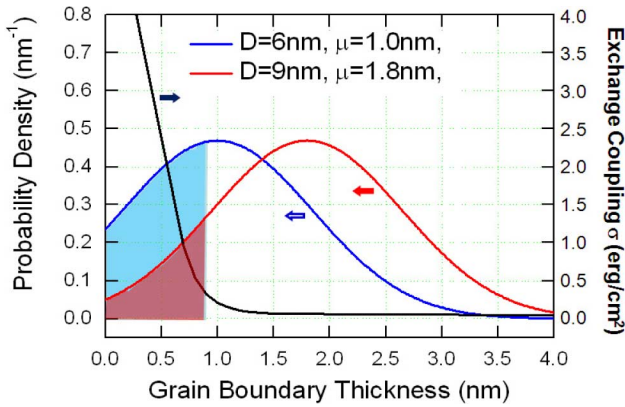


Fig. 7. The grain boundary thickness distributions used in the simulations for 6 nm grain size case (blue curve) and 9 nm grain size case (red curve). The intergranular exchange coupling strength as a function of thickness used here is obtained by numerically fitting the Cr dusting of SiOx interlayer case shown in Fig. 5.

software with media nonlinearity incorporated in the model. The head fly height is 9 nm and the vertical field magnitude in the media is about 8 kOe.

Recording of all “1s” (1T bit-patterns) have been simulated and transition profiles are obtained by averaging the simulated recorded magnetization patterns across the track width. In each case at each linear density analyzed here, approximately 200 transitions are used to maintain sufficient statistics. The medium SNR is calculated using the magnetization remanence at each linear density and the total integrated noise with cutoff frequency corresponding to 3 MFCI linear density. Fig. 7 shows two grain boundary distributions, extracted from TEM micrographs of some experimental disk media in recent years, used for the calculations. The blue curve with open circle symbols in Fig. 8 shows the calculated medium SNR as a function of linear recording density for the case of 6 nm grain diameter when the corresponding grain boundary thickness distribution (shown in Fig. 7) is used to randomly assign the intergranular exchange coupling between neighboring grain in the granular layer accordingly. The resulting mean exchange coupling field is approximately 400 Oe and the maximum coupling field is capped at 1500 Oe, corresponding to a theoretical value for zero separation between two magnetic grains. The SNR for the exact same case but assuming zero intergranular exchange coupling instead is also plotted (red curve w/triangle symbols) for comparison. At 1.5 MFCI linear density, the SNR degradation due to the random intergranular exchange coupling is approximately 6 dB.

As shown in Fig. 7, the oxide grain boundary thickness in practice often decreases significantly as one tries to reduce the grain size. If the standard deviation of grain boundary thickness distribution maintains as the case shown in the figure, the percentage of grains with grain boundary thickness below the onset thickness for the coupling increases significantly. The resulting SNR impact can be significant such that it essentially offsets the noise reduction due the grain size reduction. As shown in Fig. 9, the medium SNRs are virtually the same for the two cases with grain diameter  $D = 6$  nm and  $D = 9$  nm, respectively, with corresponding grain boundary thickness distribu-

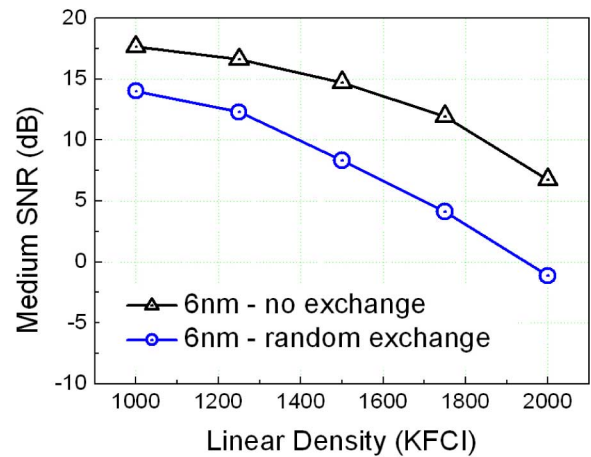


Fig. 8. *Blue curve with open circles*: Calculated medium SNR as a function of linear density using the grain boundary distribution for the 6 nm grain size case shown in Fig. 7. *Black curve with triangles*: Comparison for the same case without any intergranular exchange coupling in the granular layer.

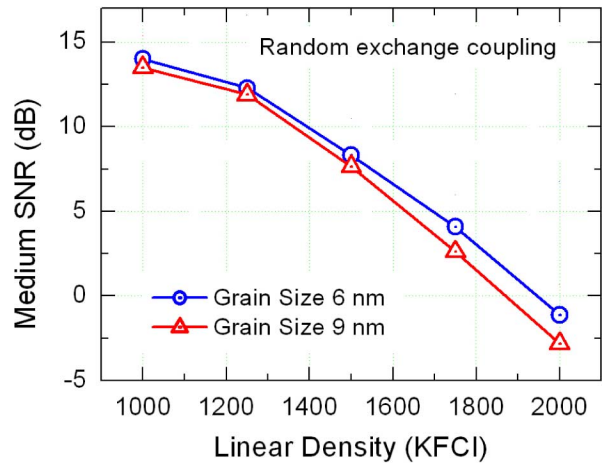


Fig. 9. Calculated medium SNR as a function of linear density for the two grain size cases using the grain boundary distributions shown in Fig. 7.

tions shown in Fig. 7. This indicates that without material improvement of the oxide grain boundaries, one needs to maintain the grain boundary thickness to be sufficiently thick while reducing grain diameter for improving medium SNR.

### III. GRAIN BOUNDARY INTERFACIAL ANISOTROPY

Strong magnetic anisotropy could arise from the interface, often referred to as surface anisotropy or interfacial anisotropy. Significant surface anisotropy at magnetic grain boundary interfaces could then be detrimental to overall perpendicular anisotropy of the grains in the granular layer. Moreover, the ratio between the grain boundary surface area and grain volume is proportional to the inverse of the grain diameter, the smaller the grain size, the greater the impact.

In order to quantitatively determine the strength of the interfacial magnetic anisotropy at the oxide/magnetic grain boundaries, a set of experiments have been performed. Using RF sputtering technique, we grow an epitaxial Cr layer with (112) texture on a single crystal MgO with (110) texture, using the same technique described in Section II of this paper. 15 [Co/Cr(6

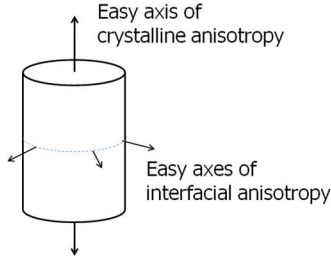


Fig. 10. Illustration of the detrimental effect by possible grain boundary interfacial anisotropy to the overall perpendicular anisotropy strength of a magnetic grain.

nm]) or [CoPt/Cr(6 nm)] bilayers are then deposited on top of the Cr underlayer in which the Co or CoPt layers show excellent (10.0) crystalline texture and Cr (112) texture. Both out of plane and in-plane magnetic hysteresis measurements are performed using a PPMS magnetometer made by Quantum Design. Since there is a single easy axis for Co or CoPt layers in the film plane due to the above epitaxial growth, two in-plane hysteresis curves are measured in the directions along and transverse to the crystalline easy axis, respectively. The integrated area of the in-plane transverse hysteresis loop, indicated by the blue shade shown in Fig. 11, measures the crystalline anisotropy energy of the Co (or CoPt) layers. The integrated area of the out-of-plane hysteresis loop, indicated by the red+blue shade measures the combined effect of crystalline anisotropy energy, the demagnetization energy and the interfacial anisotropy energy from the Co/Cr (or CoPt/Cr) interfaces. Since the effective anisotropy energy density can be written as

$$K_{\text{eff}} = K_u + 2\pi M_s^2 - \frac{2K_s}{\delta_{\text{Co,orCoPt}}} \quad (2)$$

where  $K_u$  is the crystalline anisotropy energy density,  $M_s$  is the saturation magnetization of the Co (or CoPt) layers,  $\delta$  is the thickness of each individual Co (or CoPt) layer, and  $K_s$  is the interfacial anisotropy energy density with easy axis perpendicular to the film plane. The thickness of Co (or CoPt) individual layers is varied from 12 nm to 1.5 nm to determine the value of  $K_s$ . It is found that over this thickness range, the measured saturation magnetization of the magnetic layers remains virtually the same.

Fig. 12 shows the measured ( $K_{\text{eff}} - K_u$ ) versus inverse thickness of the Co or CoPt layer for the Co/Cr and CoPt/Cr bilayer structures, respectively. By fitting a linear line to the measurement values, the interfacial anisotropy energy density can be derived, as shown in the table below the figure. The obtained surface anisotropy values for the Cr/Co interfaces are similar to those reported in previous literature [7], [8]. Comparing with the value for the Cr/Co interfaces, the value for the Cr/CoPt interfaces is slightly lower.

We also performed the same measurements for Co/oxide structure for three types of oxides: SiOx, CrOx, and TiOx. In all these cases, one Co layer with (10.0) texture is deposited on top of the Cr (112) underlayer followed by an oxide layer of 10 nm in thickness. By fitting the measured data with a line and counting the contribution of the bottom Cr/Co interfacial

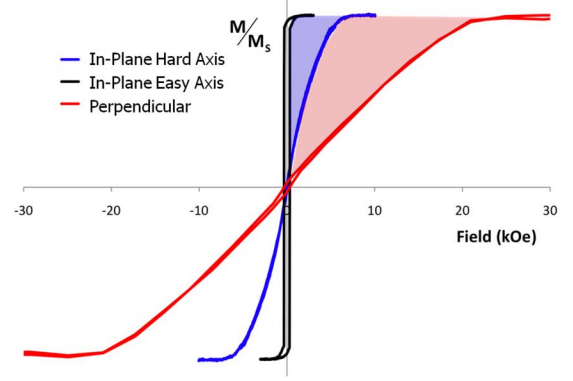
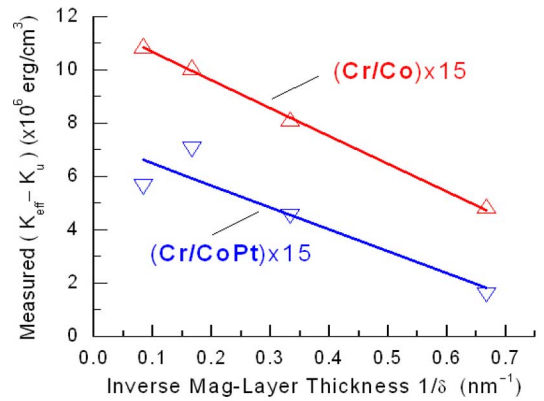


Fig. 11. A set of measured hysteresis loops of a [Co/Cr]x15 bilayer structure: in-plane easy axis loop (black), in-plane transverse loop (blue), and out-of plane perpendicular loop (red).



	Co	CoPt
$K_{s, \text{Co}(10.0)/\text{Cr}(112)}$	0.52 ergs/cm <sup>2</sup>	0.41 ergs/cm <sup>2</sup>

Fig. 12. Plots of measured  $K_{\text{eff}} - K_u$  values for [Cr/Co]  $\times$  15 (red) and [Cr/CoPt]  $\times$  15 (blue) bilayer structures. The calculated surface anisotropy energy density is plotted in the table.

anisotropy listed in Fig. 12, the derived interfacial anisotropy values for SiOx/Co, CrOx/Co, and TiOx/Co are listed in the lower right table in Fig. 13. The interfacial anisotropy value for the SiOx/Co interface is the lowest while that of the TiOx/Co interface is the highest.

Except for the SiOx/Co interface, the measured interfacial anisotropy with the easy axis parallel to surface normal all exhibit significant values. Quantitatively assessing the impact on grain switching field, Fig. 14 shows micromagnetic calculation of the switching field as a function of grain diameter for a 12 nm tall *hcp* Co grain [5]. At the measured interfacial anisotropy magnitudes, significant switching field reduction would occur especially at 8 nm grain size or below.

More importantly, if this interfacial anisotropy strongly depends on the detailed “quality” of the metal/oxide interface, it can vary significantly from grain to grain, broadening the switching field distribution. In addition, since the surface-to-volume ratio of a grain is inversely proportional to the grain diameter, or size, a distribution of grain size would also yield additional switching field distribution.

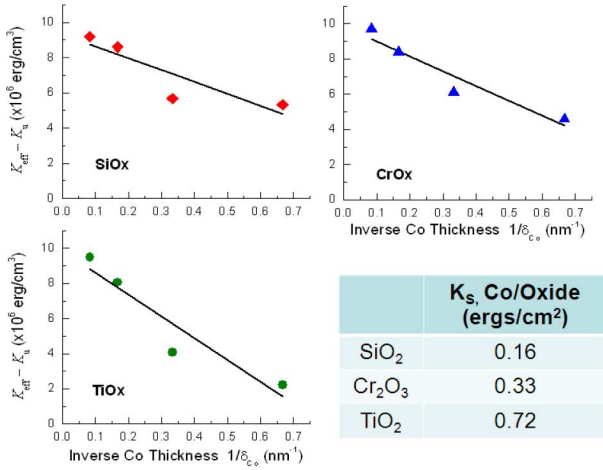


Fig. 13. Plots of measured  $K_{eff} - K_u$  values for SiOx/Co, CrOx/Co, and TiOx/Co interfaces. The derived interfacial anisotropy energy density is listed in the table. The compositions of the oxide layers listed in the table at lower right are the composition of the sputtering targets used.

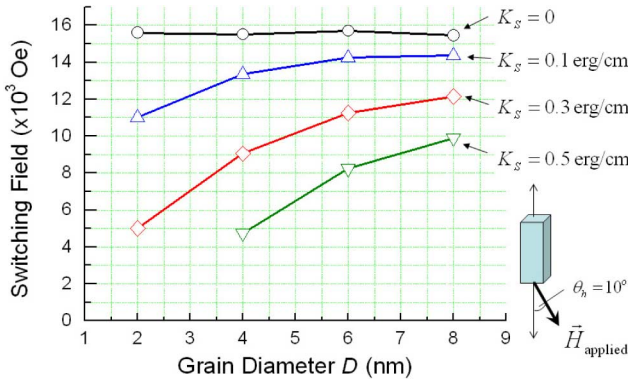


Fig. 14. Micromagnetic modeling calculation of switching field dependence on grain size for four different grain boundary interfacial anisotropy values.

#### IV. STACKING FAULTS WITHIN CO-ALLOY GRAINS

Recent experimental studies have indicated stack faults (SF) in (0002) textured *hcp* CoCrPt film can yield significant reduction of the film perpendicular crystalline anisotropy [9], [10]. Although previous experimental studies on SF in *hcp* Co-alloy film have been quite extensive [11], quantitative correlation between processing conditions and the extent of SF for the CoCrPt-Oxide granular layer in present perpendicular thin film media remains to be challenging. Furthermore, if the existence of SF proves to be significant in current disk media, quantitative understanding of how the extent of SF actually impact grain switching field would be critically important.

Fig. 15 illustrates the *fcc* and *hcp* stacking. In equilibrium, the position dependence of the second nearest neighbors (along the perpendicular stacking direction) interaction energy  $1/\delta_{Co}$  determines the type of stacking by the atoms.

During film growth by sputtering, however, the kinetics of the atoms in forming an atomic layer could yield much higher probability for forming SF in *hcp* stacking of Co-alloy than that predicted by equilibrium conditions. Four types of SF are illustrated in Fig. 16. The disruption of the ABAB *hcp* stacking by an insertion of one or more “short” ABC *fcc* stacking will result

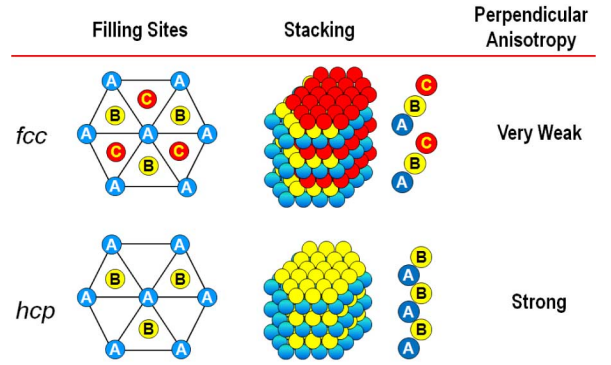


Fig. 15. Illustration of *hcp* and *fcc* stacking. (111) in a *fcc* Co film are easy axes due to negative value of  $K_1$  (cubic anisotropy energy constant), but its magnitude is over one order of magnitude lower than that of the *hcp* Co with (0002) being easy axis.

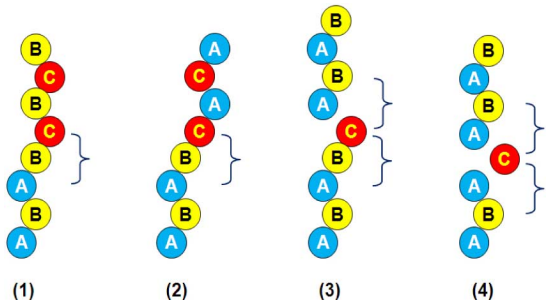


Fig. 16. Illustration of four possible types of stacking faults in *hcp* Co-alloy with (0002) texture.

in significant local reduction of crystalline anisotropy. For some of the listed SF types, the reduction of local anisotropy strength could be severe if the SF is located near the top or bottom ends of a perpendicular Co-alloy grain.

Dynamic micromagnetic modeling has been carried out to study the switching of a magnetic grain with a thin segment having reduced perpendicular crystalline anisotropy strength. Fig. 17 shows the calculated switching field reduction of Co grains of 16 nm tall and 8 nm lateral size. The results are plotted as a function of the anisotropy of a 2 nm segment in the grain for two different locations: the segment is (1) at one end of the grain (red) and (2) in the middle of the grain (2). The impact to the switching field is significantly higher if the SF is located at either the top or the bottom ends of the CoCrPt grains.

#### V. CONCLUSION AND REMARKS

Experiments have been designed and performed to obtain quantitative understanding of intergranular exchange coupling in the granular layer of present perpendicular thin film media. The dependence of the exchange coupling on the grain boundary thickness appears to be a characteristic of the oxide materials. The study also indicates that Cr segregation to the oxide grain boundaries can significantly improve exchange decoupling between adjacent grains, especially in the case of SiOx. Combined micromagnetic modeling study shows that reducing grain boundary thickness without changing/improving present oxide grain boundary materials will result in significant degradation of the medium SNR because of the random intergranular exchange

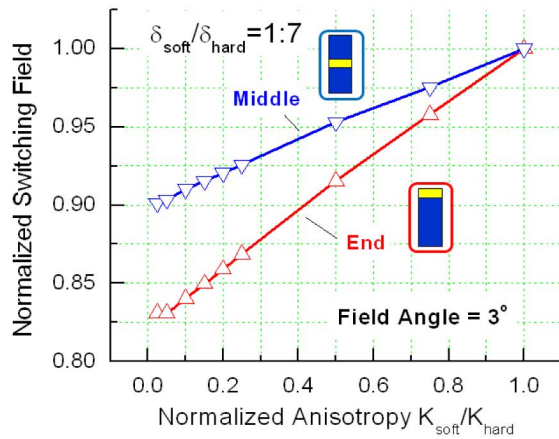


Fig. 17. Calculated switching field reduction as a function of the anisotropy strength of a 2 nm thick segment of a grain with 8 nm diameter and 16 nm tall.

coupling due to grain boundary thickness distribution below the critical thicknesses. Oxide grain boundary thickness has actually increased in recent commercial media with increased area density capability.

Interfacial anisotropy arising from oxide grain boundaries in the granular layer has also been studied for various oxide/Co, Cr/Co, and Cr/CoPt interfaces. It is found that the interfacial anisotropy is the smallest for SiO<sub>x</sub>/Co and the largest for TiO<sub>x</sub>/Co among the above measured interfaces. The magnitudes of all the measured interfacial anisotropy are significant enough to yield grain switching field reduction at present grain sizes (<8 nm).

Stacking faults within a *hcp* Co-alloy grain of (0002) texture could also yield significant switching field reduction of the grain. When the stacking faults are located at the ends of the grain, the impact to the local anisotropy strength is expected to be greater as well as the resulting magnetic switching field.

#### ACKNOWLEDGMENT

This research was supported in part by the Data Storage Systems Center at Carnegie Mellon University and its industrial sponsors, in particular Showa Denko K. K. The authors would like to thank Dr. Hiroshi Sakai-san for some of the motivating and elucidating discussions.

#### REFERENCES

- [1] Y. Sonobe, D. Weller, Y. Ikeda, K. Takano, M. E. Schabes, G. Zeltzer, H. Do, B. K. Yen, and M. E. Best, "Coupled granular/continuous medium for thermally stable perpendicular magnetic recording," *J. Magn. Magn. Mater.*, vol. 235, pp. 424–428, 2001.
- [2] G. Bertero, R. Acharya, S. Malhotra, K. Srinivasan, E. Champion, S. Lambert, G. Lauhoff, and M. Desai, in *The Magnetic Recording Conference (TMRC)*, San Diego, 2010, Paper A2.
- [3] V. Sokalski, D. E. Laughlin, and J.-G. Zhu, *Appl. Phys. Lett.*, vol. 95, 2009, 102507.
- [4] V. M. Sokalski, J.-G. Zhu, and D. E. Laughlin, "Characterization of oxide materials for exchange decoupling in perpendicular thin film media," *IEEE Trans. Magn.*, vol. 46, no. 6, pp. 2260–2263, 2010.
- [5] J.-G. Zhu, H. Yuan, S. Park, T. Nuhfer, and D. E. Laughlin, "Grain topography in perpendicular thin film media and impact of possible surface anisotropy," *IEEE Trans. Magn.*, vol. 45, no. 2, pp. 911–916, 2009.
- [6] Y. Wang and J.-G. Zhu, "Understanding noise mechanism in small grain size perpendicular thin film media," *IEEE Trans. Magn.*, vol. 46, no. 6, pp. 2391–2393, 2010.
- [7] Y. Henry, C. Meny, A. Dinia, and P. Panissod, "Structural and magnetic properties of semiepitaxial Co/Cr multilayers," *Phys. Rev. B*, vol. 47, no. 22, 1993.
- [8] Zeidler *et al.*, "Reorientational transition of the magnetic anisotropy in Co/Cr(001) superlattices," *Phys. Rev. B*, vol. 53, no. 6, 1996.
- [9] M. Takahashi and S. Saito, "Current perspectives of CoPt based granular media-materials and processes," in *PMRC 2010*, 2010, Paper 17 pA-3.
- [10] S. Saito, A. Hashimoto, D. Hasegawa, and M. Takahashi, "Semi-quantitative evaluation of stacking faults in pseudo-hcp thin films by laboratory-scale in-plane x-ray diffraction," *J. Phys. D: Appl. Phys.*, vol. 42, p. 145007, 2009.
- [11] B. Lu, T. Klemmer, K. Wierman, G. Ju, D. Weller, A. G. Roy, D. E. Laughlin, C. Chang, and R. Ranjan, "Study of stacking faults in Co-alloy perpendicular media," *J. Appl. Phys.*, vol. 91, no. 10, pp. 8025–8027, 2002.